

## Supporting Information:

### A modified cyclen azaxanthone ligand as a new fluorescent probe for zinc

Hela Nouri,<sup>a,b</sup> Cyril Cadiou,<sup>a</sup> Latévi Max Lawson-Daku,<sup>c</sup> Andreas Hauser, Sylviane Chevreux, Isabelle Déchamps,<sup>a</sup> Fabien Lachaud,<sup>a</sup> Riadh Ternane,<sup>b</sup> Malika Trabelsi-Ayadi,<sup>b</sup> Françoise Chuburu,<sup>a</sup> Gilles Lemercier<sup>a</sup>

### Table of Contents

**Figure S1 :** Excitation and emission spectra of the ligand **L** in the solid state

**Figure S2 :** Superimposed optimized geometries of **L** and  $[ZnL]^{2+}$  in the gas phase (blue) and in MeOH (red) [PBE-D3/TZP results].

**Figure S3 :** Quantum yields measurements for **L**,  $ZnL$ , and  $Zn_2L$ .

**Table S1 :** Characterization of the 30 lowest-lying singlet excited state of **L** in MeOH (SAOP/TZP results).

**Table S2 :** Characterization of the 10 lowest-lying triplet excited state of **L** in MeOH (SAOP/TZP results).

**Table S3 :** Characterization of the 10 lowest-lying singlet excited state of  $[ZnL]^{2+}$  in MeOH (SAOP/TZP results).

**Figure S4 :** Ground-state frontier molecular orbitals of **L** in MeOH (SAOP/TZP results).

**Figure S5:** Ground-state frontier molecular orbitals of  $[ZnL]^{2+}$  in MeOH (SAOP/TZP results).

**Figure S1.** Excitation and emission of the ligand L in the solid state

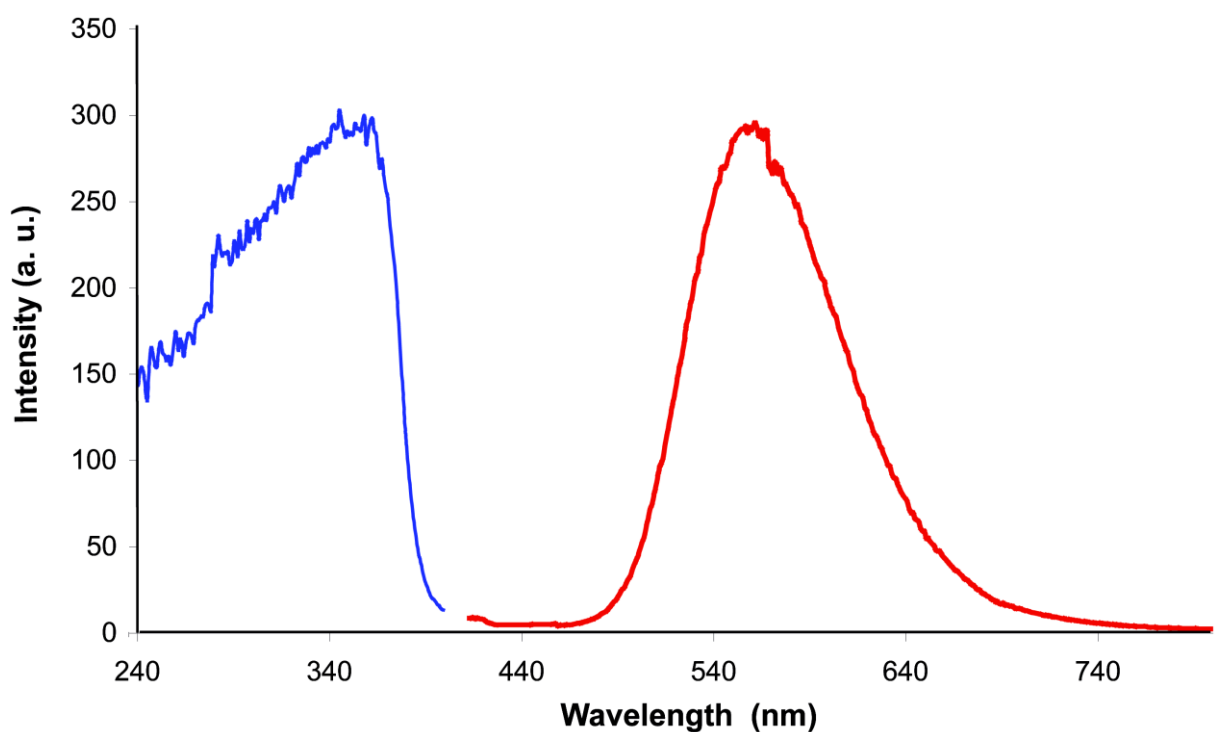


**Figure S2.** Quantum yields measurements for **L**, ZnL, and Zn<sub>2</sub>:L

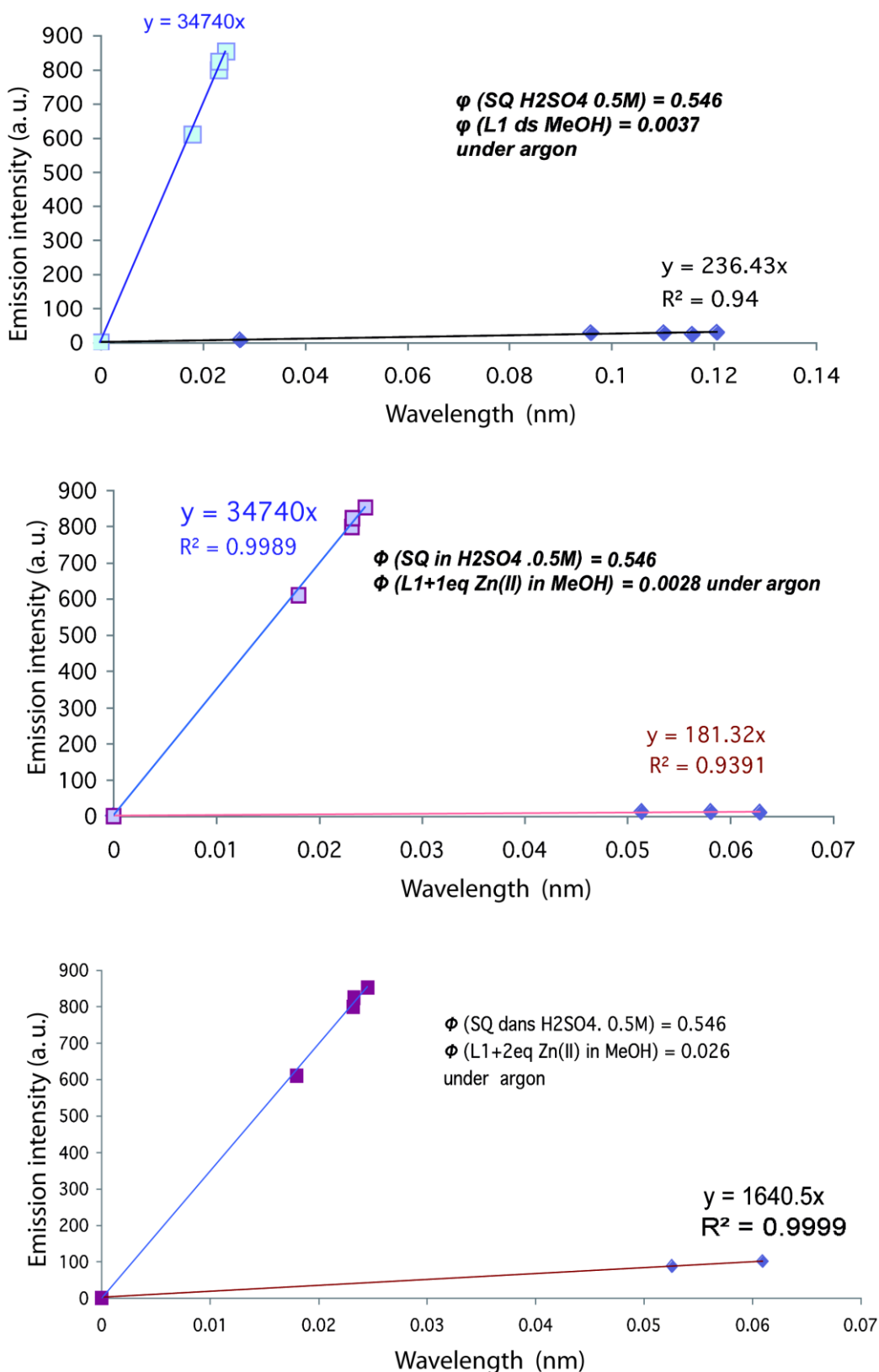


**Figure S3:** Superimposed optimized geometries of **L** and  $[\text{ZnL}]^{2+}$  in the gas phase (blue) and in MeOH (red) [PBE-D3/TZP results

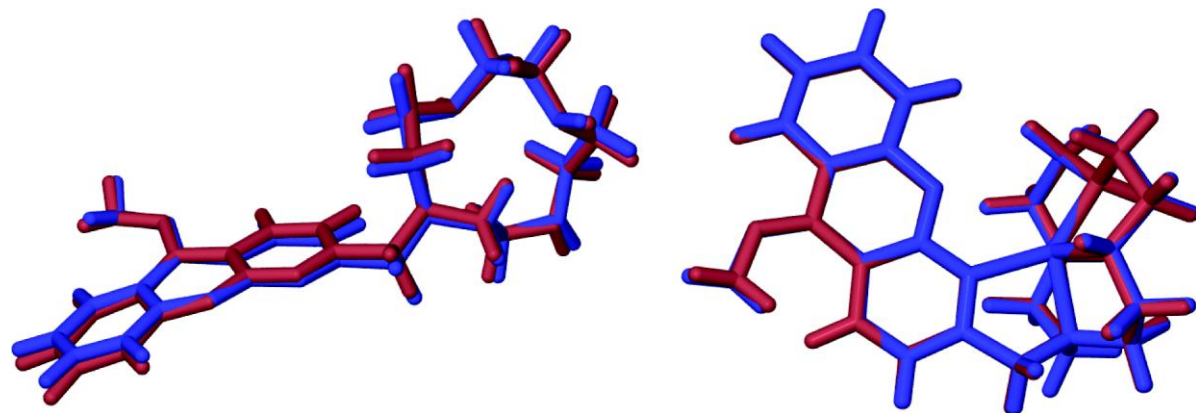


**Table S1:** Characterization of the 30 lowest-lying singlet excited state of **L** in MeOH (SAOP/TZP results).<sup>a</sup> The involved molecular orbitals are shown in Table S3.

State	Character	Energy (cm <sup>-1</sup> )	Oscillator strength (x 10 <sup>4</sup> )	Major MO → MO contributions (%)
S <sub>1</sub>	n-π* CT	17612	96	HOMO → LUMO (99%)
S <sub>2</sub>	n-π* CT	19839	30	HOMO-1 → LUMO (97%)
S <sub>3</sub>	n-π* CT	20018	2	HOMO-2 → LUMO (100%)
S <sub>4</sub>	n-π* CT	23840	37	HOMO-4 → LUMO (98%)
S <sub>5</sub>	n-π* CT	25213	44	HOMO → LUMO+1 (98%)
S <sub>6</sub>	n-π* CT	25655	46	HOMO → LUMO+2 (92%)
S <sub>7</sub>	π-π*	26090	1121	HOMO-3 → LUMO (75%)
S <sub>8</sub>	n-π* CT	27497	3	HOMO-1 → LUMO+1 (99%)
S <sub>9</sub>	n-π* CT	27714	0	HOMO-2 → LUMO+1 (100%)
S <sub>10</sub>	n-π* CT	27972	20	HOMO-1 → LUMO+2 (98%)
S <sub>11</sub>	n-π* CT	28186	1	HOMO-2 → LUMO+2 (100%)
S <sub>12</sub>		28732	22	HOMO → LUMO+3 (98%)
S <sub>13</sub>	π-π*	29937	73	HOMO-3 → LUMO+1 (74%) HOMO-6 → LUMO (11%) HOMO-3 → LUMO+2 (10%)
S <sub>14</sub>	π-π*	30472	74	HOMO-3 → LUMO+2 (60%) HOMO-5 → LUMO (26%)
S <sub>15</sub>	n-π* CT	31047	16	HOMO-1 → LUMO+3 (93%)
S <sub>16</sub>	n-π* CT	31265	1	HOMO-2 → LUMO+3 (100%)
S <sub>17</sub>	π-π*+ n-π* CT	31481	83	HOMO-5 → LUMO (44%) HOMO-4 → LUMO+1 (28%) HOMO-3 → LUMO+2 (13%)
S <sub>18</sub>	n-π* CT	31597	47	HOMO-4 → LUMO+1 (72%) HOMO-5 → LUMO (14%)
S <sub>19</sub>	n-π* CT	32048	7	HOMO-4 → LUMO+2 (97%)
S <sub>20</sub>	π-π*	34726	1308	HOMO-3 → LUMO+3 (47%) HOMO-6 → LUMO (24%)
S <sub>21</sub>	n-π*	35038	495	HOMO-8 → LUMO (75%) HOMO-6 → LUMO (16%)
S <sub>22</sub>	n-π* CT	35062	404	HOMO-4 → LUMO+3 (60%) HOMO-6 → LUMO (16%) HOMO-8 → LUMO (15%)

S <sub>23</sub>	$\pi\text{-}\pi^*$	35325	486	HOMO-4 → LUMO+3 (29%) HOMO-3 → LUMO+3 (24%) HOMO-6 → LUMO (16%) HOMO-7 → LUMO (10%)
S <sub>24</sub>	n- $\pi^*$	36157	288	HOMO-7 → LUMO (78%)
S <sub>25</sub>	$\pi\text{-}\pi^*$	37699	15	HOMO-9 → LUMO (56%) HOMO-5 → LUMO+1 (32%)
S <sub>26</sub>	n- $\pi^*$ CT	38786	16	HOMO → LUMO+4 (86%) HOMO-10 → LUMO (14%)
S <sub>27</sub>	n- $\pi^*$ CT	38832	22	HOMO-10 → LUMO (85%) HOMO → LUMO+4 (13%)
S <sub>28</sub>	$\pi\text{-}\pi^*$	39772	323	HOMO-5 → LUMO+1 (28%) HOMO-11 → LUMO (22%) HOMO-9 → LUMO (14%) HOMO-5 → LUMO+3 (14%)
S <sub>29</sub>	n- $\pi^*$ CT	40038	19	HOMO-11 → LUMO (77%)
S <sub>30</sub>	$\pi\text{-}\pi^*$	40222	3470	HOMO-5 → LUMO+2 (53%) HOMO-6 → LUMO+1 (11%)

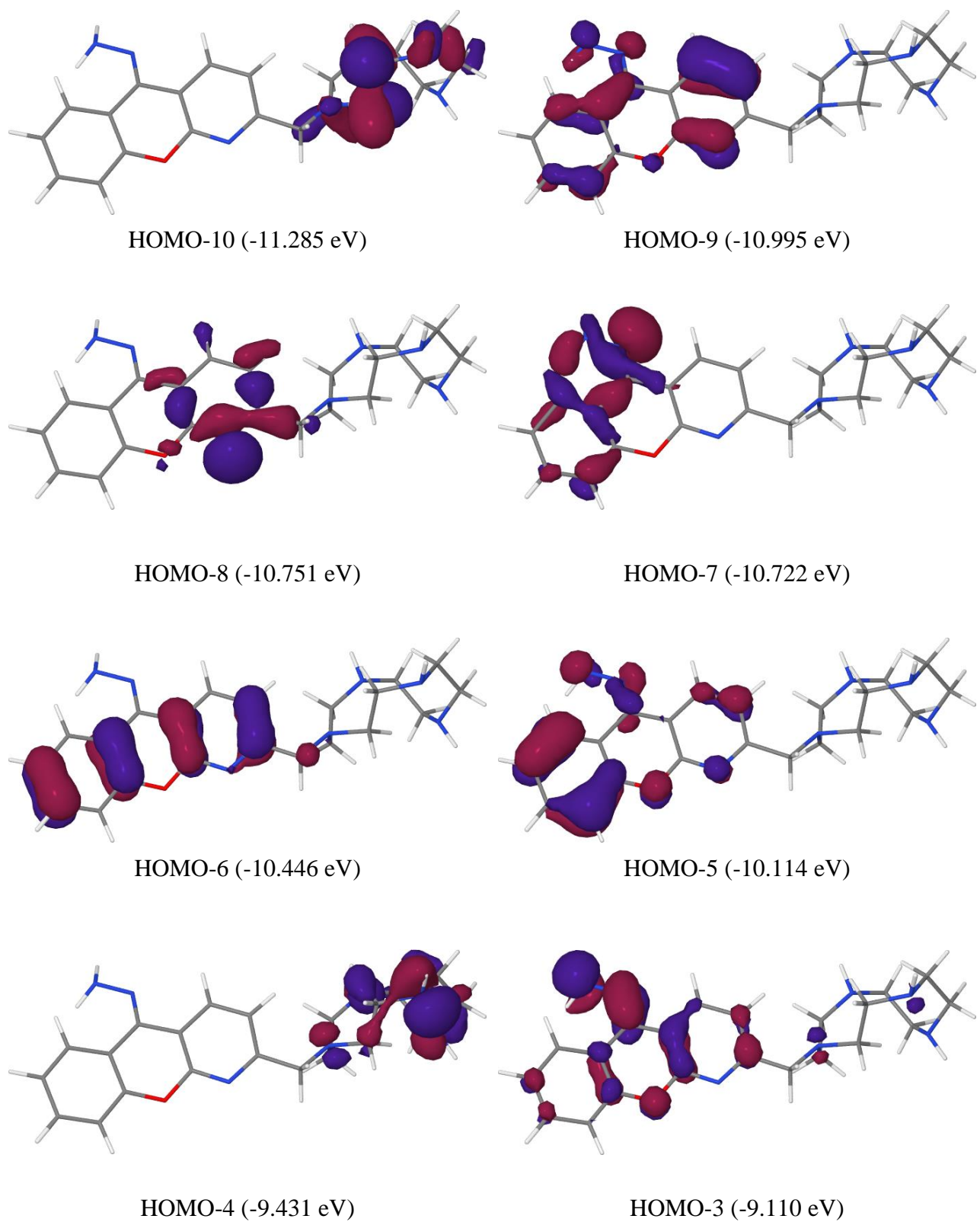
<sup>a</sup> n- $\pi^*$  CT: the S<sub>0</sub>→S<sub>n</sub> transition is a n- $\pi^*$  charge-transfer transition from the cyclen to the azaxanthone-hydrazone moiety.  $\pi\text{-}\pi^*$ : the S<sub>0</sub>→S<sub>n</sub> transition is a  $\pi\text{-}\pi^*$  transition centered on the azaxanthone-hydrazone moiety. n- $\pi^*$ : the S<sub>0</sub>→S<sub>n</sub> (n=21) transition is a n- $\pi^*$  transition localized on the azaxanthone-hydrazone fragment.

**Table S2:** Characterization of the 10 lowest-lying triplet excited state of **L** in MeOH (SAOP/TZP results).<sup>a</sup> The involved molecular orbitals are shown in Table S3.

State	Character	Energy (cm <sup>-1</sup> )	Major MO → MO contributions (%)
T <sub>1</sub>	n-π* CT	17317	HOMO → LUMO (98%)
T <sub>2</sub>	π-π* CT	19259	HOMO-3 → LUMO (60%)
			HOMO-1 → LUMO (37%)
T <sub>3</sub>	n-π* CT	19930	HOMO-1 → LUMO (62%)
			HOMO-3 → LUMO (36%)
T <sub>4</sub>	n-π* CT	20014	HOMO-2 → LUMO (98%)
T <sub>5</sub>	n-π* CT	23833	HOMO-4 → LUMO (100%)
T <sub>6</sub>	n-π* CT	25067	HOMO → LUMO+1 (99%)
T <sub>7</sub>	n-π*	25519	HOMO → LUMO+2 (99%)
T <sub>8</sub>	n-π* CT	27370	HOMO-1 → LUMO+1 (93%)
T <sub>9</sub>	n-π* CT	27708	HOMO-2 → LUMO+1 (100%)
T <sub>10</sub>	n-π* CT	27788	HOMO-1 → LUMO+2 (83%)
			HOMO-3 → LUMO+2 (12%)

<sup>a</sup> n-π\*: CT: the S<sub>0</sub>→T<sub>n</sub> transition is a n-π\* charge-transfer transition from the cyclen to the azaxanthone-hydrazone moiety. π-π\*: the S<sub>0</sub>→T<sub>n</sub> transition is a π-π\* transition centred on the azaxanthone-hydrazone moiety.

**Figure S4:** Ground-state frontier molecular orbitals of **L** in MeOH (SAOP/TZP results).



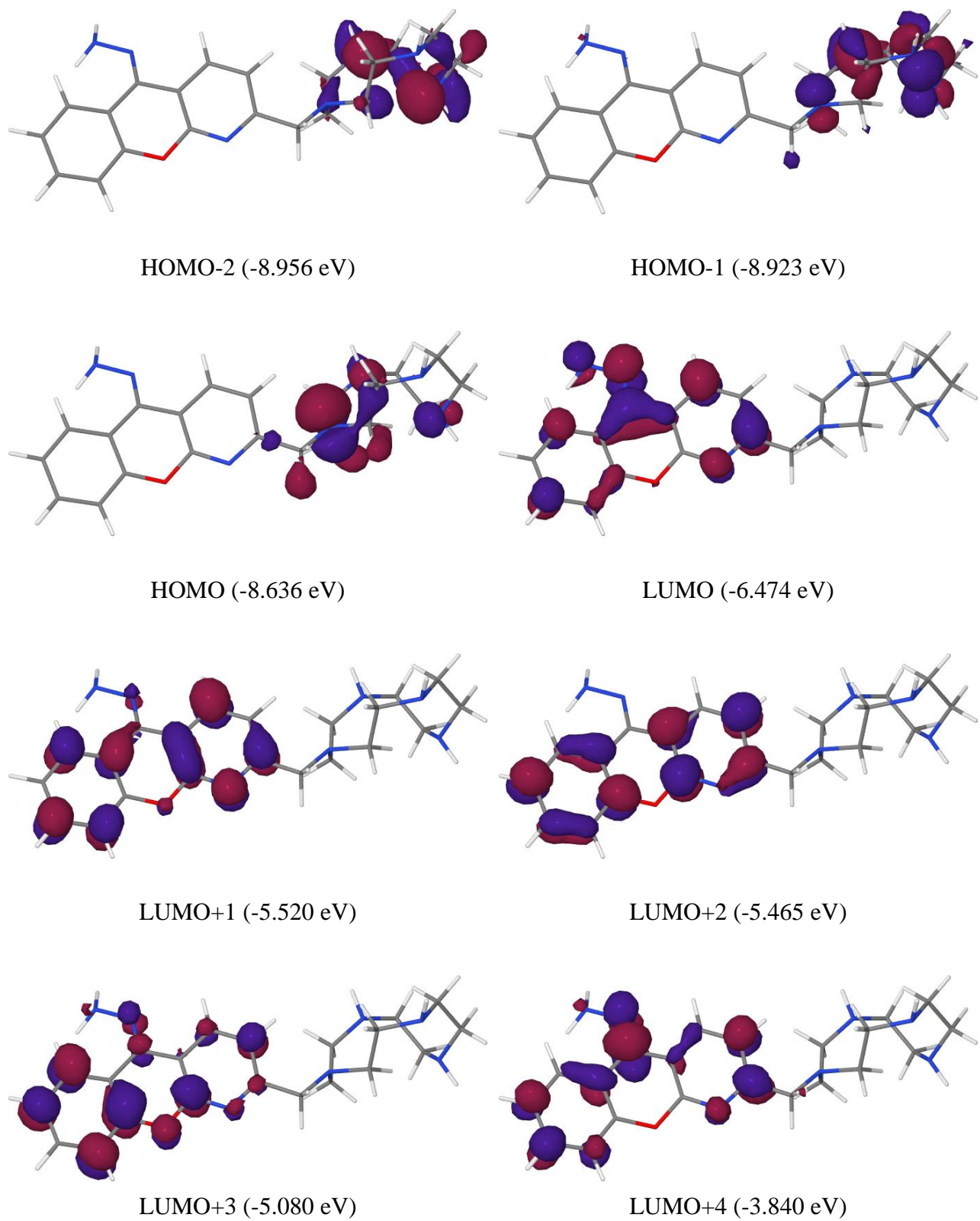
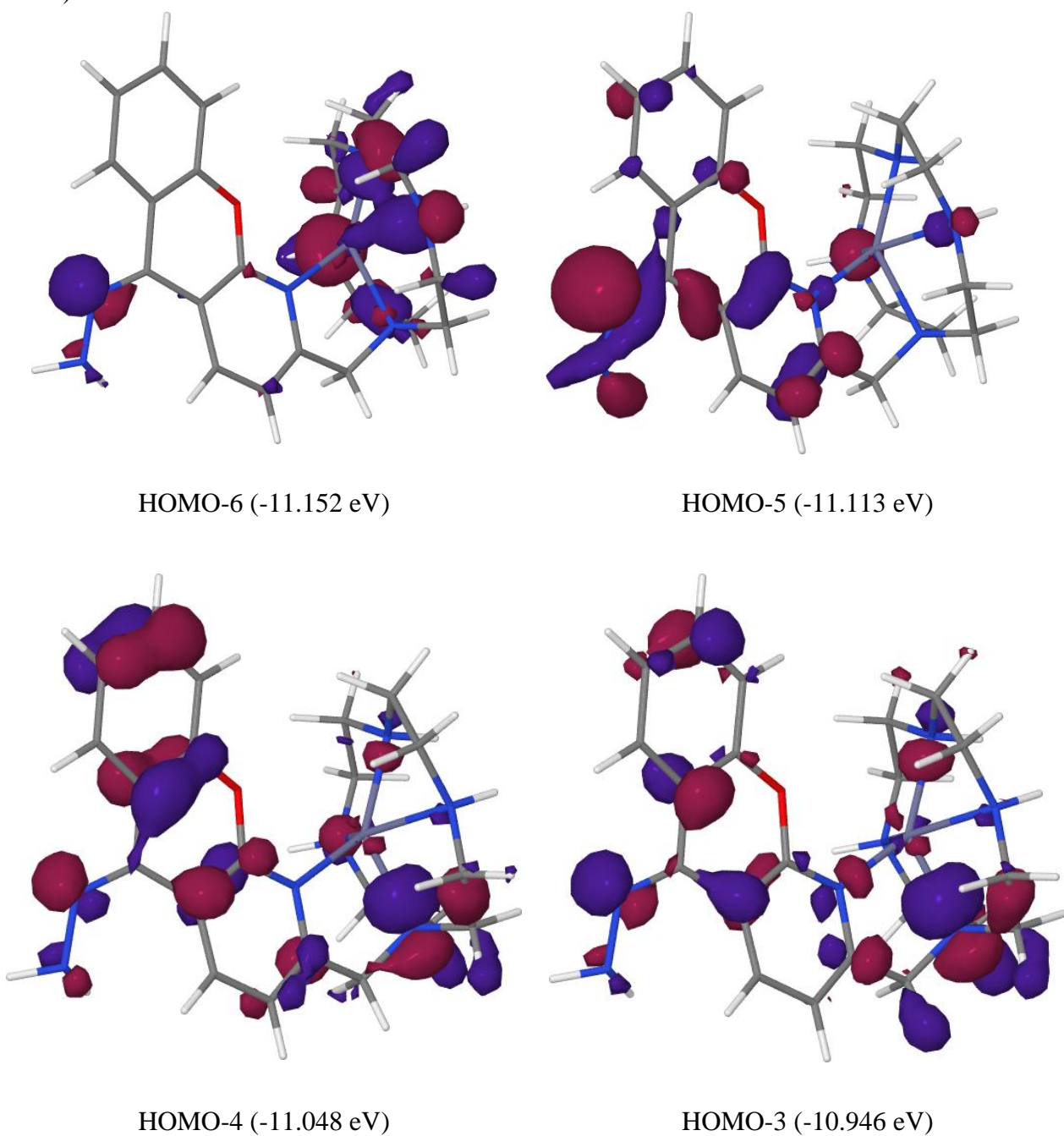


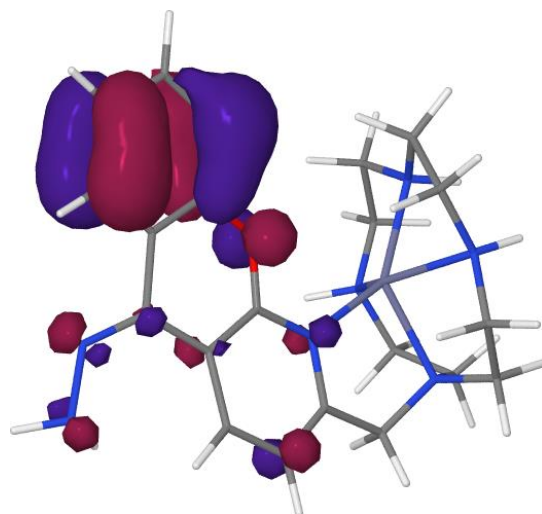
**Table S3:** Characterization of the 10 lowest-lying singlet excited state of  $[ZnL]^{2+}$  in MeOH (SAOP/TZP results).<sup>a</sup> The involved molecular orbitals are shown in Table S5.

State	Character	Energy ( $\text{cm}^{-1}$ )	Oscillator strength (x $10^4$ )	Major MO → MO contributions (%)
$S_1$	$\pi-\pi^*$	22904	604	HOMO → LUMO (83%) HOMO → LUMO+1 (10%)
$S_2$	n- $\pi^*$ CT	25629	16	HOMO-1 → LUMO (100%)
$S_3$	$\pi-\pi^*$	27441	309	HOMO → LUMO+1 (62%) HOMO-2 → LUMO (17%) HOMO → LUMO+2 (13%)
$S_4$	$\pi-\pi^*$	27846	41	HOMO-2 → LUMO (78%) HOMO → LUMO+1 (11%)
$S_5$	“admix.”	30999	168	HOMO-3 → LUMO (65%) HOMO → LUMO+2 (18%)
$S_6$	“admix.”	31385	535	HOMO → LUMO+2 (36%) HOMO-4 → LUMO (31%) HOMO-3 → LUMO (11%)
$S_7$	n- $\pi^*$ CT	31813	14	HOMO-1 → LUMO+1 (99%)
$S_8$	“admix.”	32366	103	HOMO-6 → LUMO (49%) HOMO-5 → LUMO (25%) HOMO-4 → LUMO (16%)
$S_9$	“admix.”	32894	201	HOMO-6 → LUMO (41%) HOMO-4 → LUMO (29%) HOMO-3 → LUMO (11%)
$S_{10}$	“admix.”	33981	84	HOMO-2 → LUMO+1 (44%) HOMO-5 → LUMO (33%)

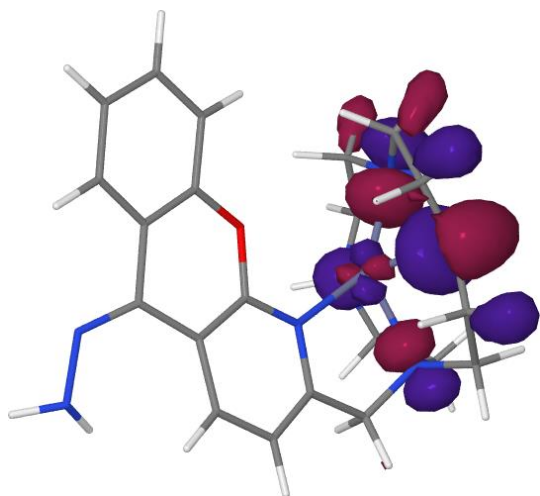
<sup>a</sup>  $\pi-\pi^*$ : the  $S_0 \rightarrow S_n$  transition is a  $\pi-\pi^*$  transition centered on the azaxanthone-hydrazone moiety. n- $\pi^*$  CT: the  $S_0 \rightarrow S_n$  transition is a n- $\pi^*$  charge-transfer transition from the cyclen to the azaxanthone-hydrazone moiety. “admix.”: while the virtual orbitals involved in the MO → MO contributions are  $\pi^*$  centered on the azaxanthone-hydrazone moiety, the occupied orbitals extend over the whole molecule with varying contributions from the lone pairs of the nitrogen atoms of the hydrazone and cyclen fragments (see Table S5).

**Figure S5:** Ground-state frontier molecular orbitals of  $[ZnL]^{2+}$  in MeOH (SAOP/TZP results).

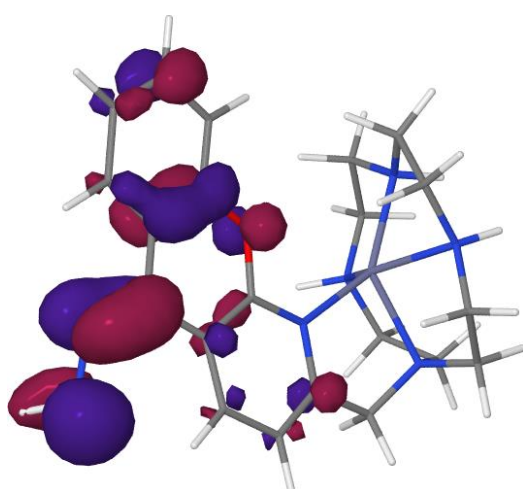




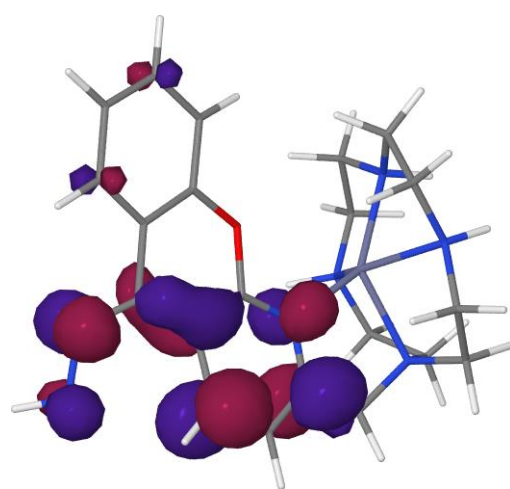
HOMO-2 (-10.489 eV)



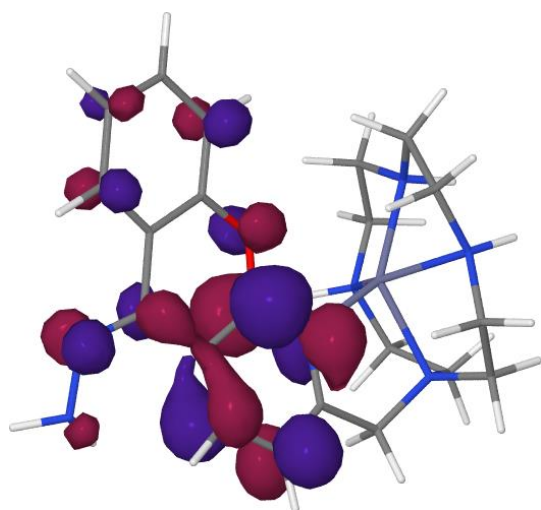
HOMO-1 (-10.306 eV)



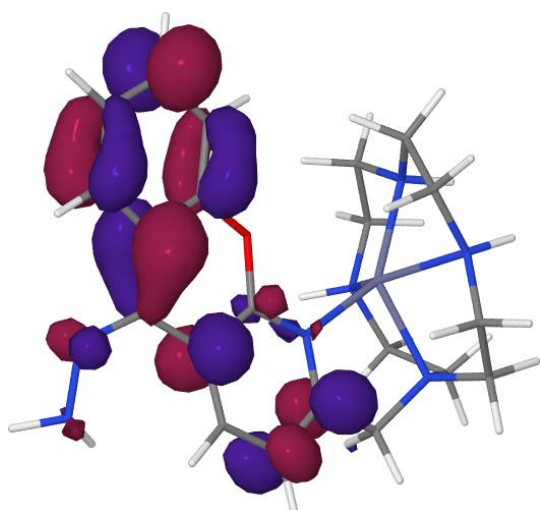
HOMO (-9.535 eV)



LUMO (-7.137 eV)



LUMO+1 (-6.368 eV)



LUMO+2 (-5.987 eV)